Energy for Sustainability International Conference 2017
Designing Cities & Communities for the Future
Funchal, 8-10 February, 2017

THERMAL MANAGEMENT OF PHOTOVOLTAICS WITH THERMAL ENERGY STORAGE UNITS FILLED WITH MICROENCAPSULATED PCMS

N. Soares[1,2]*, P. Antunes[1], A.R. Gaspar[1], J.J. Costa[1]

1: ADAI, LAETA, Department of Mechanical Engineering, University of Coimbra, Coimbra, Portugal.
*e-mail: nelson.soares@dem.uc.pt
2: ISISE, Department of Civil Engineering, University of Coimbra, Coimbra, Portugal

Keywords: Phase change materials, PCM, Photovoltaics, Thermal regulation, Effective heat capacity.

Abstract *High operating temperatures reduce the performance of photovoltaic (PV) devices by reducing the efficiency of solar to electrical energy conversion in the PV cells. This paper presents a numerical study based on the effective heat capacity method to evaluate the thermal performance of a PV system incorporating a thermal energy storage unit filled with a microencapsulated phase change material (PCM) – Micronal® DS 5001 X. The PCM module is intended to control the temperature rise in the PV cells. The main goal of this work is to find the ideal thickness of the PCM module for the climatic conditions of Coimbra, Portugal, and to evaluate how the thermal regulation potential of PCMs (during phase change) can be used to improve the performance of the PCM-enhanced system (PV/PCM). By comparing the temperature time evolutions in the cells of the PV/PCM and the conventional PV systems, an effective thermal regulation of the PV/PCM system was observed from 6am to 3pm. Therefore, it is concluded that TES units filled with microencapsulated PCMs can be used to improve the energy performance of PV systems by reducing high operating temperatures due to solar irradiation. It was also concluded that, for the studied conditions, the ideal thickness of the PCM module was about 3.3 cm, thus increasing the energy performance of the system up to 0.8%..*

1. INTRODUCTION

PCMs are materials that undergo melting/solidification at a nearly constant temperature, storing/releasing great amounts of energy due to the latent heat involved in the solid-liquid phase change processes. Therefore, PCMs are very suitable for thermal energy storage and thermal management applications as reviewed by Soares *et al.* [1]. PV devices are a good example of systems where such effects can improve the overall performance. It has been claimed that the performance of a PV system can be improved by placing a PCM module on the panels back to passively lower the high peak operating temperatures due to solar irradiation. Some of these studies were recently reviewed by Ma *et al.* [2], Du *et al.* [3], Browne *et al.* [4] and Makki *et al.* [5]. Hasan *et al.* [6] also reviewed the main pros and cons of different thermal control techniques for building integrated PV systems, including the one with PCMs.

The PCM modules to be placed on the panels back are typically made of a high-conductivity internally-finned container used to accommodate the PCM and to avoid liquid leakage. The macrocapsule can be the only way of containment, or the PCM can be further microencapsulated before filling the container. The main advantage of using microencapsulated PCMs is that the problem of liquid leakage during manufacturing, assembling and operation can be reduced. When dealing with microencapsulated PCMs, the numerical modelling of the heat transfer with phase change becomes simpler, as the advection phenomena in the melted domain can be neglected [7] and the energy conservation equation (in its purely diffusive form) is the only governing equation to be solved.

This paper presents a transient one-dimensional numerical model developed in a homemade FORTRAN program to investigate the thermal performance of a PCM-enhanced PV system (PV/PCM). Indeed, the main goal of this work is to assess how the thermal regulation potential of PCMs can be used to reduce high operating temperatures due to solar irradiation. This work also aims to find the optimum thickness of the PCM module to be integrated in the PV/PCM system for the climatic conditions of Coimbra, Portugal.

2. PHYSICAL PROBLEM

Fig. 1 shows a sketch of the physical domain with the main heat transfer mechanisms in the PV/PCM system. The temperature in the PV cells is estimated by considering the thermal energy exchange of the PV/PCM system with the environment, and the thermal storage capacity of the PCM module. Four heat transfer mechanism are shown in Fig. 1: conduction within the PV/PCM system, convection in the front and back surfaces of the PV/PCM system, solar irradiation and energy lost by radiation from the front surface of the system to the "cold sky". I_{sol} is the daily evolution of the solar irradiation on a south-facing 35° inclined plane, and T_{amb} represents the daily evolution of the ambient temperature during the 15$^{\mathrm{th}}$ of August in Coimbra. Both variables are calculated using the Portuguese climatic database of SOLTERM®. Further information about the irradiation model considered can be found in ref. [8]. The heat transfer coefficient h_2 is considered constant and equal to 4 $\mathrm{W{\cdot}m^{-2}{\cdot}K^{-1}}$. The heat transfer coefficient h_1 is defined by Eq. (1),

where k_{air} is the thermal conductivity of the air and L_{PV} is the height of the PV module.

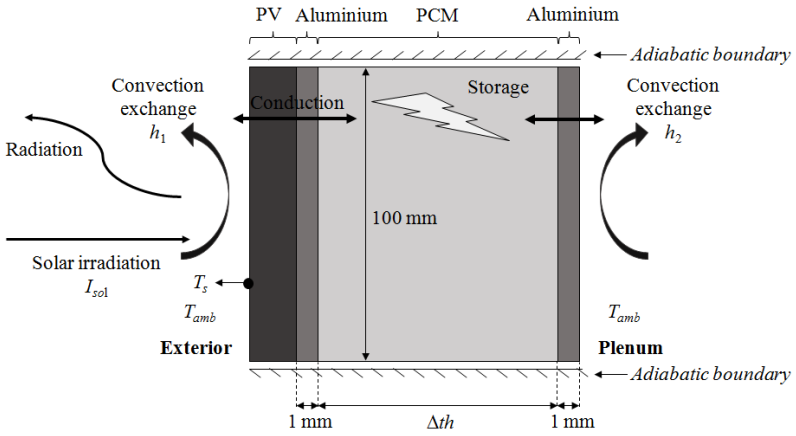

Figure 1. Sketch of the physical domain with the relevant heat transfer mechanisms in the system.

$$h_1 = \frac{Nu\, k_{air}}{L_{PV}} \tag{1}$$

The Nusselt number, *Nu*, is estimated from the empirical correlation for natural convection over a flat plate as shown in Eq. (2) [9], where *Ra* and *Pr* are the dimensionless Rayleigh and the Prandtl numbers, respectively.

$$Nu = \left\{ 0.825 + \frac{0.387\, Ra^{1/6}}{\left[1 + (0.492/Pr)^{9/16}\right]^{8/27}} \right\}^2, \tag{2}$$

$$\text{with } Ra = \frac{g \cos(90-\gamma)\, \beta_{air} (T_s - T_{amb}) L_{PV}^{\,3}}{\tau_{air}\, \alpha_{air}} \text{ and } Pr = \frac{c_{p\,air}\, \mu_{air}}{k_{air}}.$$

T_s is the instantaneous temperature on the front surface of the system, g is the gravitational acceleration (9.81 m·s^{-2}) and β_{air} is the thermal expansion coefficient. α_{air}, c_{pair}, τ_{air} and μ_{air} are the thermal diffusivity, the specific heat, the kinematic and dynamic viscosities of air, respectively, and γ is the inclination angle of the surface. The air thermophysical properties are estimated for four different ranges of the bulk temperature given in Table 1, as proposed by Kibria *et al.* [9]. The bulk temperature, T_b, is defined as $T_b = (T_s + T_{amb}) / 2$. The instantaneous T_s is obtained from the energy balance on the surface of the PV/PCM system given by Eq. (3), where ε is the emissivity (assumed 0.9), σ is the Stefan-Boltzmann constant, Δx is the distance between the surface and the first inner grid node of the PV module, and $T_{i,j}$ is the temperature in the latter. The sky temperature is defined by the Swinbank equation [10]: $T_{sky} = 0.037536\, T_{amb}^{\,1.5} + 0.32\, T_{amb}$.

Table 1. Air properties estimated for different bulk temperature ranges [9].

Properties	T_b (10–20) ºC	T_b (20–40) ºC	T_b (40–60) ºC	T_b > 60 ºC
ρ_{air} [kg·m^{-3}]	1.293	1.205	1.127	1.067
c_{pair}[J·kg^{-1}·K^{-1}]	1005	1005	1005	1009
k_{air} [W·m^{-1}·K^{-1}]	0.0243	0.0257	0.0271	0.0285
τ_{air} [m^2·s^{-1}]	0.00001330	0.00001511	0.00001697	0.0000189
β_{air} [K^{-1}]	0.0035	0.0033	0.0031	0.0029

$$I_{sol} = \varepsilon \sigma \left({T_s}^4 - {T_{sky}}^4 \right) + h_1 \left(T_s - T_{amb} \right) + k_{glass} \frac{\left(T_s - T_{i,j} \right)}{\Delta x} \quad (3)$$

The PV module is considered as a six layers system as proposed by Kibria *et al*. [9] and Armstrong and Hurley [11]. Properties of each layer are listed in Table 2.

Table 2. Properties of the six layers of the PV module. Adapted from refs. [9,11].

Layer	Thickness [m]	k [W·m^{-1}·K^{-1}]	ρ [kg·m^{-3}]	c_p [J·kg^{-1}·K^{-1}]
Glass	3×10^{-3}	1.8	3000	500
ARC	1×10^{-7}	32	2400	691
PV cells	2×10^{-4}	148	2300	677
EVA	5×10^{-4}	0.35	960	2090
Rear contact	1×10^{-7}	237	2700	900
Tedlar	1×10^{-4}	0.2	1200	1250

To evaluate the influence of the PCM module in the improvement of the energy conversion efficiency of the PV system, the time evolution of temperatures in the PV cells of the PV/PCM and the conventional PV systems will be compared. Then, the linear expression for the PV efficiency proposed by Dubey *et al.* [12] (Eq. (4)) will be used. In Eq. 4, η_{ref} is the energy conversion efficiency of the system at a reference temperature, T_{ref}, and ξ_{ref} is the temperature coefficient.

$$\eta = \eta_{ref} \left[1 - \xi_{ref} \left(T_{PVcells} - T_{ref} \right) \right],\ T_{ref} = 25\,^{\circ}\mathrm{C},\ \eta_{ref} = 0.12 \text{ and } \xi_{ref} = 0.0045\,^{\circ}\mathrm{C}^{-1}. \quad (4)$$

3. MATHEMATICAL MODEL AND NUMERICAL SOLUTION

The numerical model is based on the solution of the energy conservation equation, under purely diffusive conditions, and uses the effective heat capacity method to account for the latent heat of the solid-liquid phase change processes. The one-dimensional heat conduction equation with phase change, expressed in Cartesian coordinates can thus be written as:

$$\rho\ c_{eff}\left(T\right) \frac{\partial T}{\partial t} = \frac{\partial}{\partial x} \left(k \frac{\partial T}{\partial x} \right). \quad (5)$$

The main feature of the effective heat capacity method is that the temperature is the only dependent variable to find. Moreover, the method allows using the same

governing equation for both solid and liquid phases, avoiding the need to track the melting front position to solve the problem. Indeed, the melting/solidification fraction at each CV of the PCM domain (for each time step) is obtained as a function of the temperature calculated at the considered time step. The key in the implementation of the method lies in the approximation used for the effective heat capacity term in Eq. (5). As suggested by Al-Saadi and Zhai [13], minimal data provided by PCM manufacturer can be used to approximate the heat capacity of the PCM using a simple direct relationship with the introduction of a fictitious melting temperature range (ΔT_m), which is not known *a priori*. A rectangular-type approximation of the evolution of the effective heat capacity with temperature is sketched in Fig. 2a. This means that the effect of the latent heat of fusion is artificially modelled by a large effective heat capacity over the phase change temperature interval. In the numerical model, this high value of the effective heat capacity will block the increase (or decrease) of temperature during phase change.

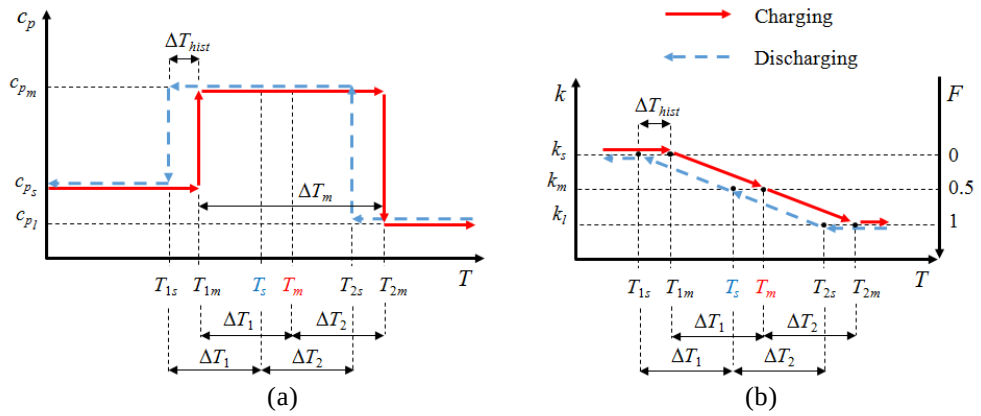

Figure 2. (a) Sketch of the effective heat capacity method considering a rectangular approximation for the variation of the effective heat capacity with temperature. (b) Sketch of the evolution of both the thermal conductivity, *k*, of the PCM and the fraction of melted PCM, *F*, with temperature.

Eq. (6) presents the definition of the effective heat capacity method for the phase change temperature interval during the charging process. The c_{pm} term reveals that, during phase change, the effective heat capacity of the PCM is directly proportional to the latent heat L and inversely proportional to the temperature interval for phase change ΔT_m. T_{1m} is the temperature when the PCM begins melting and T_{2m} is the temperature when the PCM is completely melted. The method can easily deal with the supercooling phenomenon occurring during solidification. Fig. 2 illustrates the impact of hysteresis, ΔT_{hist} (for instance caused by supercooling), in the effective heat capacity approximation. In discharging processes, T_m must be replaced by T_s in Eq. (6). Indeed, subscripts *m* and *s* refer to melting and solidification, respectively. Another important feature of the method is the flexibility to adjust the approximation of the effective heat capacity by considering different values of ΔT_1 and ΔT_2. Furthermore, these values can be different for the charging and discharging processes. Additional information about the implementation of the effective heat capacity method can be found in refs. [8,14].

$$c_p(T) = \begin{cases} c_{p_s} & T \le T_{1m} \\ c_{p_m}, & T_{1m} < T < T_{2m} \\ c_{p_l} & T \ge T_{2m} \end{cases} \text{, with } c_{p_m} = \frac{L}{\Delta T_m} + \frac{c_{p_s} + c_{p_l}}{2}. \quad (6)$$

The following assumptions are made in the present numerical study: (*i*) conduction is the only mode of heat transfer within the PV/PCM system; (*ii*) the PCM is completely solid at the beginning of simulations; (*iii*) the thermophysical properties of the materials are independent of temperature; however, for the PCM, c_p and k are different for the solid and liquid phases and k varies linearly with temperature during phase change (Fig. 2b); (*iv*) the fraction F of melted PCM at each CV is a function of the calculated instantaneous temperature (Fig. 2b); (*v*) the effect of expansion/contraction of the PCM during the phase change is neglected, and a constant ρ-value is considered for both phases; (*vi*) the materials are homogeneous and isotropic; (*vii*) $\Delta T_1 = \Delta T_2 = 2$ ºC and $\Delta T_{hist} = 1$ ºC. The main thermophysical properties of the PCM and aluminium are listed in Table 3.

Table 3. Thermophysical properties of the materials.

	T_m [ºC]	ΔT_{hist} [ºC]	ρ [kg·m^{-3}]	L [kJ·kg^{-1}]	c_p [J·kg^{-1}·°C^{-1}]	k [W·m^{-1}·°C^{-1}]
PCM	25.7	1	995	110	2478 (solid) 1774 (liquid)	0.17 (solid) 0.15 (liquid)
Aluminium	–	–	2707	–	896	204

The partial differential equation is discretized using the finite-volume method proposed by Patankar [15], with a fully implicit formulation. For the heat fluxes at the faces of each control volume (CV), the temperature gradients are approached by finite-differences and the harmonic mean is used to interpolate the thermal conductivity values at the CV interfaces. A preliminary study was conducted to evaluate the influence of the time and spatial discretizations on the numerical solutions [8]. A regular mesh of 390 inner nodes (CV dimension of 0.1 mm, along x) was adopted for the simulations together with a time step of 10 s. The set of algebraic discretization equations is solved using a tri-diagonal matrix algorithm (TDMA). At each time step, convergence is declared when the normalized sum of the absolute values of the residuals of the discretized equations is lower than 5×10^{-4}.

The numerical model was validated using the experimental results provided by Soares *et al.* [7,16]. Further information about the study carried out for the validation of the numerical model can be found in ref. [8].

4. RESULTS AND DISCUSSION

To find the best thickness of the PCM module, Δth, for the climatic conditions of Coimbra (15th of August), Portugal, a parametric investigation was performed considering Δth of 3, 3.3, 3.5 and 4 cm. Fig. 3 shows the corresponding time evolutions predicted for the total melted fraction of PCM, F_t, in the PV/PCM system during 24 hours. By definition, insufficient thermal storage is achieved when the PCM volume neither totally solidifies

nor melts during a daily cycle. On the other hand, the higher the volume of PCM, the higher the stored/released energy during a charging/discharging cycle, and the higher the thermoregulation period achieved in the PV/PCM system. Therefore, the best thickness of the PCM module would be the one that allows the volume of PCM to be completely melted during the day, and completely solidified during the night (before the beginning of a new charging period). Considering this, the results of the simulations show that Δth of 3.3 cm is the best thickness to be considered.

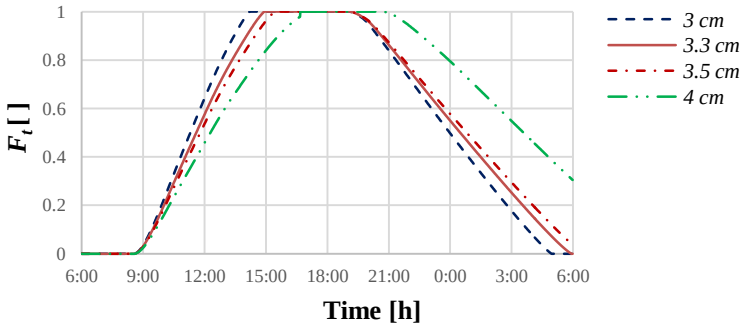

Figure 3. Time evolution of the total melted fraction of PCM, F_t, during 24 hours for different thicknesses of the PCM module.

Fig. 4a shows the time evolution of the temperature in the PV cells, $T_{PVcells}$, of the reference (PV) and the PCM-enhanced (PV/PCM) systems during 24 hours, considering Δth = 3.3 cm. Results show that PCMs are an effective way to limit the temperature rise in the PV cells from 6am to 3pm. Fig. 4b shows the time evolutions of η for the PV and PV/PCM systems during this period. In can be seen that the energy conversion efficiency of the PV system can be increased up to 0.8% by considering the PCM module on the panels back.

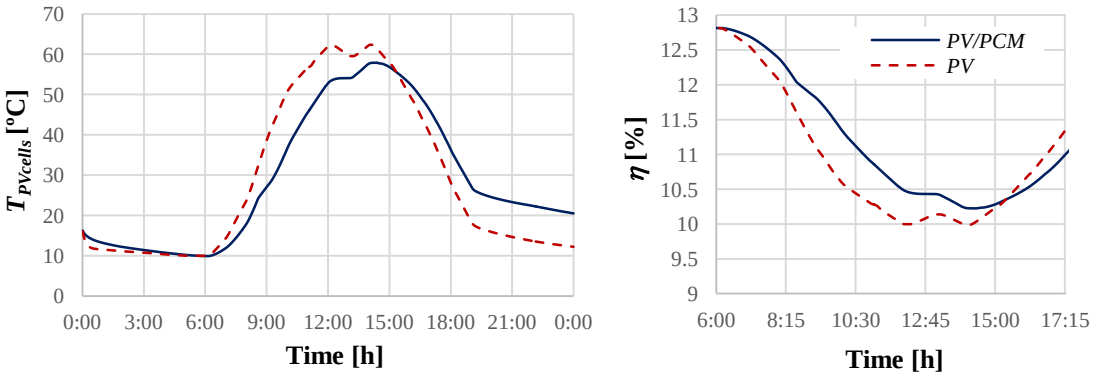

Figure 4. Time evolutions of (a) the temperature in the PV cells, $T_{PVcells}$, of the reference (PV) and PCM-enhanced (PV/PCM) systems during 24 hours, and (b) electrical efficiency of the systems, η, between 6am and 5pm (Δth = 3.3 cm).

5. CONCLUSION

This paper numerically evaluates how a PCM module can improve the thermal performance of a PV device for the climatic conditions of Coimbra, Portugal. A purely diffusive transient one-dimensional numerical model (based on the effective heat capacity method) was developed to assess the control of the temperature rise in the PV cells of the PV/PCM system, and to estimate the improvement of the electrical efficiency of the PCM-enhanced device. It is concluded that microencapsulated PCMs (placed on the panels back) are an effective means of limiting the temperature rise in the PV device (from 6am to 3pm) thus increasing the energy conversion efficiency up to 0.8% (for a 3.3 cm thick PCM module).

ACKNOWLEDGEMENTS

This project has been financed by FEDER funds through the COMPETE 2020-Operational Programme for Competitiveness and Internationalization (POCI), and by Portuguese funds through FCT in the framework of the project POCI-01-0145-FEDER-016750 | PTDC/EMS-ENE/6079/2014.

REFERENCES

[1] N. Soares, J.J. Costa, A.R. Gaspar and P. Santos, “Review of passive PCM latent heat thermal energy storage systems towards buildings' energy efficiency”, *Energy and Buildings* Vol. 59, pp. 82–103, (2013).

[2] T. Ma, H. Yang, Y. Zhang, L. Lu and X. Wang, “Using phase change materials in photovoltaic systems for thermal regulation and electrical efficiency improvement: a review and outlook”, *Renewable and Sustainable Energy Reviews* Vol. 43, pp. 1273–1284, (2015).

[3] D. Du, J. Darkwa and G. Kokogiannakis, “Thermal management systems for Photovoltaics (PV) installations: a critical review”, *Solar Energy* Vol. 97, pp. 238–254, (2013).

[4] M.C. Browne, B. Norton and S.J. Mccormack, “Phase change materials for photovoltaic thermal management”, *Renewable and Sustainable Energy Reviews* Vol. 47, pp. 762–782, (2015).

[5] A. Makki, S. Omer and H. Sabir, “Advancements in hybrid photovoltaic systems for enhanced solar cells performance”, *Renewable and Sustainable Energy Reviews* Vol. 41, pp. 658–684, (2015).

[6] A. Hasan, S.J. McCormack, M.J. Huang and B. Norton, “Evaluation of phase change materials for thermal regulation enhancement of building integrated photovoltaics”, *Solar Energy* Vol. 84 (9), pp. 1601–1612, (2010).

[7] N. Soares, A.R. Gaspar, P. Santos and J.J. Costa, “Experimental study of the heat

transfer through a vertical stack of rectangular cavities filled with phase change materials", *Applied Energy* Vol. 142, pp. 192–205, (2015).

[8] P. Antunes, *Estudo numérico de unidades de armazenamento de energia térmica com materiais de mudança de fase para a termorregulação de painéis fotovoltaicos*, Master thesis in Mechanical Engineering, Universidade de Coimbra, (2016).

[9] M.A. Kibria, R. Saidur, F.A. Al-Sulaimana and M.M.A. Aziz, "Development of a thermal model for a hybrid photovoltaic module and phase change materials storage integrated in buildings", *Solar Energy* Vol. 124, pp. 114–123, (2016).

[10] W.C. Swinbank, "Long-wave radiation fom clear skies", *Q.J.R. Meteorol. Soc.* Vol. 89, pp. 339–348, (1963).

[11] S. Armstrong and W.G. Hurley, "A thermal model for photovoltaic panels under varying atmospheric conditions", *Applied Thermal Engineering* Vol. 30 (11–12), pp. 1488–1495, (2010).

[12] S. Dubey, J.N. Sarvaiya and B. Seshadri, "Temperature dependent photovoltaic (PV) efficiency and its effect on PV production in the world – a review", *Energy Procedia* Vol. 33, pp. 311–321, (2013).

[13] S.N. AL-Saadi and Z.(J.) Zhai, "Modeling phase change materials embedded in building enclosure: a review", *Renewable and Sustainable Energy Reviews* Vol. 21, pp. 659–673, (2013).

[14] N. Soares, P. Antunes and J.J Costa, Effective heat capacity method to simulate heat difusion problems with phase change, in: Energy for Sustainability International Conference 2017, Designing Cities & Communities for the Future, Funchal, 8-10 February, 2017.

[15] S.V. Patankar, *Numerical heat transfer and fluid flow*, Washington, DC: Hemisphere Publishing Corporation, (1980).

[16] N. Soares, A.R. Gaspar, P. Santos and J.J. Costa, "Experimental evaluation of the heat transfer through small PCM-based thermal energy storage units for building applications", *Energy and Buildings* Vol. 116, pp. 18–34, (2016).